IEL2-I-06-03

Internship Report

Presented to:
Universidad de Los Andes

To obtain the degree of:
Electronic Engineering

By

Sergio Andrés Andraus Robayo

This work was done at the department of electronics of the
Ecole Nationale Supérieure des Télécommunications de Bretagne

Precoded Iterative OFDM system

Supervised by:
Charlotte Langlais, Ph.D.

July of 2006

Acknowledgements

First and foremost, I wish to thank my supervisor, Dr. Charlotte Langlais, for giving me the opportunity of working at this marvelous institution, for guiding me and giving me so much of her time, and for sharing her knowledge with me. Secondly, I thank Mario Castillo, whose work and effort are the basis of the results obtained during this internship. I wish to thank all of the Department of Electronics at the ENST Bretagne for welcoming me and making me one of their own; more particularly, I would like to express my gratitude to Dr. Claude Berrou, Dr. Sylvie Kerouédan and Dr. Christophe Jégo for their time and kindness, to Catherine Blondé and Bernard L'Hostis for their hard work and assistance and to all of the other members of the department for their company, help and friendship.

I would like to thank the Universidad de Los Andes for allowing me to spend this last semester at the ENST Bretagne through their exchange program. For their help and support during the period before this exchange semester, I wish to thank Yadira Mogollón at the Centro de Trayectoria Profesional and Dr. Néstor Peña at the Electronics Department, for without their help it would have been impossible for me to do this work at the ENST Bretagne.

To all of my family, my girlfriend and my closest friends, I wish to express my gratitude for their patience and inconditional support.

Finally, I want to thank God for guiding me and giving me the strength needed to get this far and the will to go on in the future.

Table of contents

Summary

PAPR in OFDM systems is an extensively studied problem that has effects on the power circuitry of emitters and on the maximum power required by them. In this internship report, the PAPR problem is briefly studied along with a pair of techniques that aim to solve it. The first one, signal clipping and filtering, shows a great reduction of PAPR at the expense of system performance. The second one, linear precoding, shows a modest reduction of PAPR while leaving the system performance unchanged over a Gaussian channel. The combination of the two techniques yields a slightly better performance than the one obtained through clipping and filtering alone.

Focusing on the receiver, iterative estimation and cancellation of clipping noise is first implemented on a clipped and filtered OFDM signal, yielding promising results over a Gaussian channel. On the other hand, the performance of a system using an iterative treatment of linear precoding is tested on a clipped OFDM signal, and results showing a fair robustness against the effects of clipping are obtained over a multipath fading Rayleigh channel.

Finally, a new receiver combining these two iterative techniques is proposed as a conclusion of this work, and future testing work on this system is left for future study.

Introduction

Modern communications have seen the rise of wireless communication networks as one of its most important achievements, and it is now present in everyday life, from cell phones to wireless peripherals for computers. During the past few years, Wireless Local Area Networks, or WLANs, have become a good example of the fast development of wireless communication technologies, achieving transmission of digital data at rates in the order of tens of megabits per second (IEEE 802.11g-compliant WLANs can achieve transfer rates of about 50Mbit/s).

This is no particularly easy feat to achieve considering the channel to be used. For example, a coaxial cable is a fairly reliable channel that can be easily known and characterized; air, on the other hand, is not. In order to make air a sufficiently reliable channel for digital data transmission at high rates there are various issues to solve. These issues are, among others, multipath fading and restricted use of the electromagnetic spectrum assigned for the particular application in question.

Multipath fading arrives when, as an emitter sends data to a receiver, the electromagnetic wave containing the information finds obstacles and walls on the way. The effect is that the receiver detects not only the direct path message, but also the faded copies produced by reflection from these obstacles and walls. This is an important source of inter-symbol interference (ISI) which sets a lower bound on the symbol time. In other words, in order to avoid ISI in the easiest possible way, symbols are to be sent at a rate that will guarantee that all previous symbols have disappeared from the channel before sending the next one.

To achieve high transmission rates in a multipath channel, there are a few options to be considered: one of them is to use a single-carrier modulation scheme complemented by a proper equalization stage; the second is to use multiple carrier waves so that symbols can be sent "in parallel" to their destination, always respecting the lower bound on symbol time. In this work, the focus will be set on the latter. However, considering the possible constraints on allocated bandwidth for other applications, it is desirable to use a limited amount of bandwidth. To solve this problem, a multiple carrier scheme called Orthogonal Frequency Division Multiplexing (OFDM) was developed [1]; it uses a series of closely spaced subcarrier frequencies in order to limit its use of available bandwidth, hence solving the problem.

Some other problems arise when a wireless transmission channel is frequency-selective. If this frequency selectivity were to cut off one or many of the subcarrier frequencies, then the mapped symbols sent through them would be completely lost. A way of solving this problem is to partially send symbols through different subcarrier frequencies. In other words, if we were to send a linear combination of mapped symbols through each frequency instead of just one, when frequency selectivity strikes the sent information will not be completely lost. In this way, the concept of linear precoding [2] is introduced into OFDM modulation.

OFDM has a drawback, however: when data is sent using this modulation scheme, waveforms with very large power peaks that have a low probability of occurrence may -and eventually will- appear. The effect of these power peaks is direct on the power circuitry of the emitter, as the linear range of power amplifiers is, of course, limited, and hence distortion appears. However, if this problem were to be solved solely by the power circuitry, not only would the amplifier be overdimensioned considering the average power of the sent signal, but problems concerning power regulations might appear. Therefore, a way to modify OFDM signals in such a way that their large power peaks won't appear without sacrificing the communication system's performance must be sought.

A quantity called Peak to Average Power Ratio is the quantity to be reduced in the problem outlined in the last paragraph. As its name implies, it is defined as the peak power in an OFDM symbol divided by its mean power. In this internship report, a brief summary of OFDM and the PAPR problem are first presented in chapter 1 to give way to a presentation of a pair of PAPR reducing techniques, namely signal clipping and filtering and linear precoding of mapped symbols in chapters 2 and 3. As clipping and filtering a signal has effects on the system's performance, chapter 4 is devoted to testing a technique to attenuate those effects in the OFDM receiver and mixing it with linear precoding to see whether an improvement in performance can be achieved. In the same chapter, an iterative linear precoding treatment technique's performance when handling clipped OFDM signals is tested. Finally, conclusions and future perspectives on this work are presented after this last chapter.

Chapter 1

OFDM and the PAPR problem

Orthogonal Frequency Division Multiplexing is the modulation of choice for digital wireless communication systems. As stated previously, it is a multi-carrier modulation scheme, and in the first section of this chapter the possible constraints will be considered and a logical construction of OFDM will be presented. In the following sections, the Peak to Average Power Ratio will be defined and the behavior of OFDM in terms of PAPR will be presented, to finally show the origins of the drawbacks of OFDM modulation.

1.1 Construction of a multiple carrier modulation scheme

A wireless communication channel has a certain inherent characteristic that makes high transmission rates difficult: multiple paths. This is an important source of inter-symbol interference, and must be dealt with appropriately either through equalization or a multiple carrier wave scheme of transmission. The first removes ISI while the second avoids it by transmitting symbols for a sufficiently long time. In this work, the focus is set on the latter strategy.

As an emitter sends data to the receiver using electromagnetic waves, it is not only the original emitted wave that reaches it, as there are other reflected copies that come from objects present between the two. In a real-life situation, between the emitter and the receiver there will be obstacles like buildings, walls and other objects that will make the wave reflect. The result is the arrival of the main wave front followed by a series of attenuated replicas. For a later arrival there will be a stronger attenuation. If the symbol time is short enough, a newly sent symbol will find interference from the reflected waveforms produced by the preceding symbol. A way out of this problem might be that of using a larger constellation for the mapping of the signal and stretching the symbol time. However, performance might be hurt since it's easier to make mistakes at the time of estimation of the sent symbols when a larger constellation comes into the picture. With this in mind, the most efficient way of achieving a large transfer rate without making use of equalization would be through the use of multiple carriers.

Let us imagine that a sequence of N symbols are to be sent via N subcarrier frequencies and that, in the end, all of these modulated symbols are added up and sent. The time representation of this scheme is, then,

$$x(t) = \sum_{k=0}^{N-1} X_k e^{j2\pi f_k t}, \tag{1.1}$$

where X_k is the k-th mapped symbol and f_k is the k-th subcarrier frequency. Let us suppose, furthermore, that the subcarrier frequencies are equally separated from each other, and that they are integer multiples of the symbol rate, $1/T$, where T is the OFDM symbol time, not to be confused with the mapped symbol time (the OFDM symbol time divided into the number of mapped symbols in it), T/N. The above equation then becomes

$$x(t) = \sum_{k=0}^{N-1} X_k e^{j2\pi \frac{kt}{T}}, \tag{1.2}$$

which resembles a Fourier series. If this signal were to be sampled N times per symbol time (that is, at $\frac{nT}{N}$), the sampled signal would then be

$$x_n = \sum_{k=0}^{N-1} X_k e^{j2\pi \frac{kn}{N}}, \tag{1.3}$$

and this expression is the same as that of an Inverse Discrete Fourier Transform (IDFT), with the exception of a coefficient of $N^{-1/2}$. This is the (discrete) time representation of the signal generated by the mapped symbols. The remarkable resemblance of this expression to the one for a DFT is worth giving some thought to. In a multiple carrier system, a series of oscillators and filters would have to be used at the output of the transmitter, along with an adder to completely build it, yet this equation shows that this can be avoided by using an IDFT and then using a filter to go back from equation 1.3 to equation 1.2. In this way, the only issue left to solve is how to use this signal in continuous time (as in eq. 1.2) at the receiver for demodulation. An OFDM symbol will be limited in time by a window function such as the one below.

$$w(t) = \begin{cases} 1 & \text{if } |t| \leq 1/2 \\ 0 & \text{otherwise} \end{cases}$$

From this expression, we find the continuous time representation of the transmitted OFDM symbol after filtering.

$$s(t) = \frac{1}{\sqrt{N}} w\left(\frac{t}{T}\right) \sum_{k=0}^{N-1} X_k e^{j2\pi \frac{kt}{T}} \tag{1.4}$$

This last expression includes the missing scaling factor from the IDFT, and can be converted into the frequency domain through a Fourier transform to give

$$S(f) = \frac{T}{\sqrt{N}}\text{sinc}(\pi f T) \star \sum_{k=0}^{N-1} X_k \delta\left(f - \frac{k}{T}\right) = \frac{T}{\sqrt{N}} \sum_{k=0}^{N-1} X_k \text{sinc}(\pi T f - \pi k). \tag{1.5}$$

Here, $\star$ denotes the convolution product. It must be noted that, if f is chosen equal to l/T, with l an integer such that $0 \leq l \leq N-1$ (the subcarrier frequencies), the sinc function above becomes a Kronecker delta function and we get $TN^{-1/2}X_l$. This means that the mapped symbols in different subcarrier frequencies do not interfere amongst themselves, which is the reason for the "Orthogonal" in OFDM. The signal carrying the OFDM symbol is then sampled at the receiver at a rate T/N. Since $s(t)$ has a period of T, the window function does not have an effect on the sampling process, and the sampled signal can be written as

$$s_n = \frac{1}{\sqrt{N}} \sum_{k=0}^{N-1} X_k e^{j2\pi \frac{kn}{N}}. \tag{1.6}$$

Here, an ideal noiseless transmission has been assumed for the purpose of illustration. This expression corresponds exactly to the IDFT of X_k, and it suffices to take the DFT of s_n to retrieve the mapped symbols X_k from the signal.

The above calculations are the core of OFDM modulation. It is surprising that a multicarrier modulation scheme can be constructed with DFTs at its core, reducing hardware complexity and cost and allowing a significant increase in transfer rate for a wireless communications system. It is customary to extend the OFDM symbol time through the insertion of a "guard interval", which is achieved by repeating (partially) the signal assigned to the OFDM symbol using the fact that it is periodic, so that the continuity of the send signal is maintained and so that we make sure that the ISI is kept at bay. It goes without saying that all parameters are kept unchanged, the guard interval only repeats the signal, but it has no effects on the receiving portion of the system.

A simplified diagram of an OFDM system is shown below.

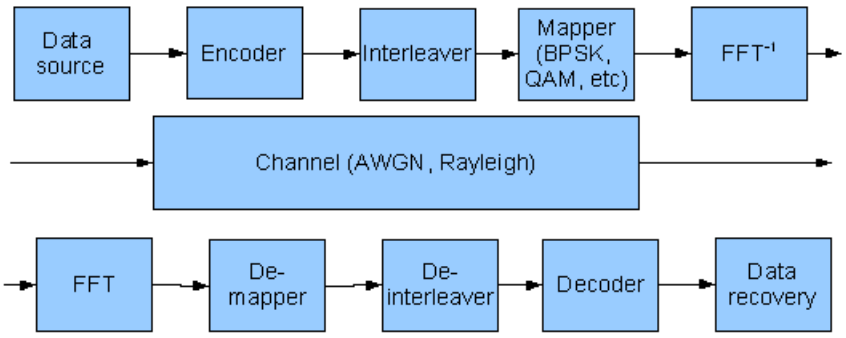

Figure 1.1. A simplified OFDM transmission chain. Right before and after the channel are the DFTs who provide the core for this type of modulation. Some details, like transmission filters and guard interval insertion, are implicit while others are made explicit for the first time.

Figure 1.1 depicts a simplified OFDM transmission chain. Undiscussed stages of this chain are the encoding/decoding stage and the interleaving/deinterleaving stage. As binary data comes from the data source it is encoded via channel coding, like block codes or convolutional encoding (in the present work we will use the latter). This provides data a larger robustness against errors. Also, before a packet of information is broken up into OFDM symbols, it is interleaved randomly so that error bursts are spread along various symbols in such a way that the channel decoder will have a larger probability of correcting errors introduced by the channel. This transmission chain has been designed for a WLAN environment, and hence realistic testing and simulations are done using a block-fading multipath channel model, though a first approach is done through an Additive White Gaussian Noise channel for preliminary testing.

As far as the use of bandwidth is concerned, we must ensure that OFDM modulation can be used in a limited frequency support. It has been shown by Le Masson [3] that the secondary lobes outside the band of interest have an amplitude of less than 0.2 times the average amplitude in the allocated band, which is about 7dB of attenuation. This guarantees that no other bands will be significantly affected by these secondary lobes thereby showing that an OFDM-based wireless network can coexist with other wireless networks using other frequency bands.

From the above discussion, it can be seen that OFDM is a very powerful modulation scheme that solves the ISI problem and that respects the assigned band of frequencies. However, OFDM has one drawback, which is its very large Peak to Average Power Ratio (PAPR), as will be seen on the next section.

1.2 The PAPR problem

The PAPR for a given OFDM symbol is defined as the maximum attained power divided by its mean power, as shown in the following formula.

$$\mathrm{PAPR}(\boldsymbol{x}) = \frac{\max_{0\leq k\leq N-1}\left(|x_k|^2\right)}{N^{-1}\sum_{k=0}^{N-1}|x_k|^2} \tag{1.7}$$

Here, $\boldsymbol{x}$ is the vector of the discrete-time values of the OFDM symbol and, as before, N is the number of subcarriers. This definition is straightforward and easily applicable. Let us find the worst possible case of PAPR for OFDM, which is when only one element of $\boldsymbol{x}$ is nonzero and the rest are equal to zero. This situation arises only when the mapped symbol sequence is of the form $X_k = \lambda e^{j\phi k}$, where λ is an arbitrary complex amplitude and $e^{j\phi}$ is a rotation applied k times to λ. When choosing the rotation angle, we must be careful not to fall out of the constellation. In other words, we are looking for sequences in which every symbol lies on a circle of radius $|\lambda|$ and has a phase difference of ϕ with the preceding and following symbols. This represents a sequence with only one component in

the time domain. The most simple of these sequences is the one arising from $e^{j\phi} = 1$, and in that case,

$$x_n = \frac{1}{\sqrt{N}} \sum_{k=0}^{N-1} \lambda e^{j2\pi nk/N} = \begin{cases} \dfrac{\lambda}{\sqrt{N}} & \text{if } n = 0 \\ 0 & \text{otherwise} \end{cases}, \tag{1.8}$$

and therefore, the PAPR for this sequence is

$$\text{PAPR}(\vec{x}) = \frac{\frac{\lambda^2}{N}}{\frac{\lambda^2}{N^2}} = N. \tag{1.9}$$

This means that, in the worst case, a 64-subcarrier OFDM scheme can have a PAPR of 64. Considering the 3 most common constellations of symbols (BPSK, QPSK and 16QAM), the probability of occurrence of these power surges can be calculated. As an example, let us consider the QPSK constellation, in which all symbols lie on a circle centered at the origin. We can choose $\lambda = e^{j\pi/4}$, $e^{j3\pi/4}$, $e^{-j\pi/4}$ or $e^{-j3\pi/4}$, while ϕ can be chosen to be $0, \pi$ or $\pm\pi/2$. For any combination of λ and ϕ a valid worst-case sequence can be found, and hence there are 16 possible worst-case sequences for QPSK. Using a similar reasoning, one can find that there are 4 worst-case possibilities for BPSK, and using the fact that 16QAM is a combination of 4 QPSK modulations either enlarged or rotated, we find that for this last constellation there are 64 worst-case possibilities. The probability of occurrence of any one of these sequences is $(N_s^{-1})^N$, where N_s is the number of symbols in the constellation. The total probabilities of a worst-case sequence for these 4 constellations are, then,

$$\begin{aligned} 4\left(\frac{1}{2}\right)^N &= 2^2\left(\frac{1}{2}\right)^N \;\rightarrow\; \text{BPSK}, \\ 16\left(\frac{1}{4}\right)^N &= 2^4\left(\frac{1}{2}\right)^{2N} \;\rightarrow\; \text{QPSK and} \\ 64\left(\frac{1}{16}\right)^N &= 2^6\left(\frac{1}{2}\right)^{4N} \;\rightarrow\; \text{16QAM}. \end{aligned}$$

It can be directly seen that, as the number of subcarriers grows larger, the probability of a worst case drops. However, avoiding the worst case through the enlargement of N is not feasible, since the complexity of the system rises considerably due to the Fast Fourier Transforms necessary to implement an OFDM communication system.

With these results, the fact that very large power peaks occur with low probability in OFDM transmissions has been shown. Through extensive modulation, a broader perspective on PAPR can be achieved. The steps are the following: first, a large number of OFDM symbols is calculated, then their PAPR is measured and finally the ratio of OFDM symbols with PAPR larger than a given value to the total number of OFDM symbols is calculated. The resulting function is the Complementary Cumulative Distribution Function (CCDF) for PAPR. Castillo [4] outlined a proof of the following theoretic CCDF stated by Han and Lee [5]:

$$P(\text{PAPR} > z) = 1 - (1 - e^{-z})^N. \tag{1.10}$$

N is still the number of subcarriers, and z is the PAPR value being compared. The following figure shows how this theoretic calculation matches the simulated results.

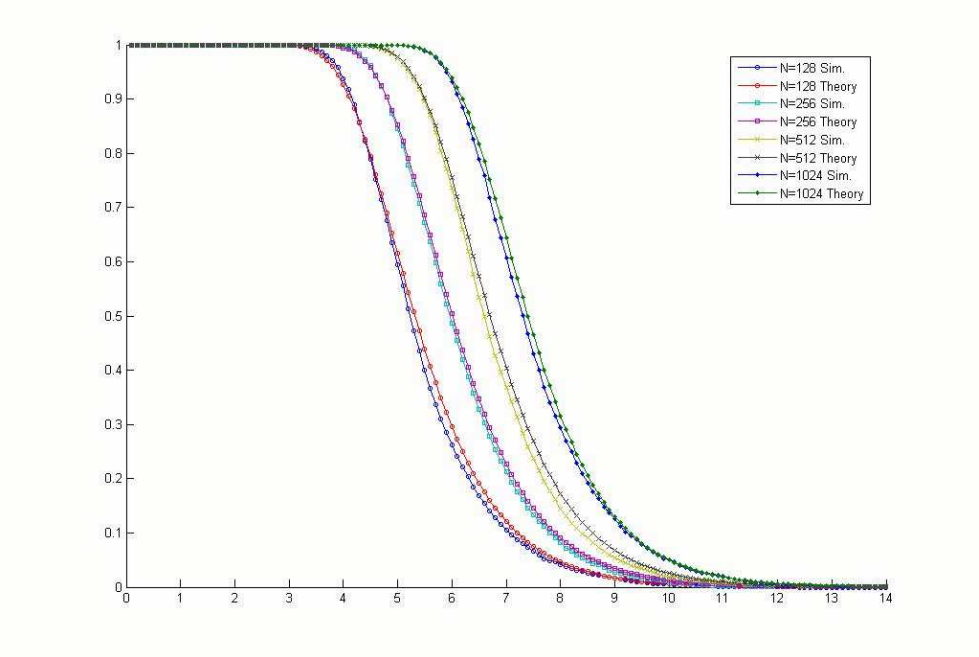

Figure 1.2. CCDF of PAPR for a given number of subcarrier frequencies. On the x axis, the possible values of PAPR are shown, while the y axis represents the probability of finding a PAPR larger than the value considered in x. Both axes are dimensionless. (Taken from [4])

It was found above that the probability for the worst case was smaller as N became larger, but remembering the result in eq. 1.9, we see that the worst-case PAPR grows linearly with the number of subcarrier frequencies. This means that as N is chosen larger, the largest PAPR grows as well and it has a nonzero probability, a fact that can be confirmed by looking at figure 1.2, in which the curves corresponding to a larger N are shifted to the right of those corresponding to lesser values of N. From this graph, it can be deduced that at least half of the OFDM symbols produced for $N = 128$ have a PAPR larger than 5, that is, there is a peak five times larger than the mean power in the symbol.

These large power peaks pose no problem in theory, where there is no limit to how much instantaneous power can be put into a signal, but in practice this is not the case. Power amplifiers used in transmission are not ideal, of course, and hence the power they can give to a signal has a limit. If these amplifiers were to be designed considering the worst case, they would turn out to be overdimensioned since the largest possible power peaks have a very low probability of arising, and conversely, if the power circuitry is designed to have a low maximum power, then the OFDM signal would be distorted and the information in it would be damaged. These are the consequences of the PAPR problem in OFDM; the following chapters will be devoted to reducing the PAPR of an OFDM signal while keeping the system's performance unchanged.

Chapter 2

The clipping technique

2.1 Description and effects on PAPR

A simple and straightforward way of reducing PAPR is by clipping the OFDM signal to some maximum amplitude. This amplitude, of course, must be defined relative to the average signal power, since PAPR is what we want to control. As proposed by Ochiai and Imai [6], the Clipping Ratio (CR) is a quantity defined by

$$\gamma = \frac{A_{\max}}{\sqrt{P_{\text{ave}}}}. \tag{2.1}$$

In other words, the CR is defined as the ratio of the maximum allowed signal amplitude to the square root of the signal's average power. Once a clipping ratio is chosen as the main parameter for signal clipping, and after a signal's average power is measured, the maximum allowed amplitude for the signal is found and clipping is then done. The output of such a "clipping" block is

$$x_{\text{out}}(t) = \begin{cases} x_{\text{in}}(t) & \text{if } |x_{\text{in}}(t)| \leq A_{\max} \\ A_{\max} e^{j \arg(x_{\text{in}}(t))} & \text{otherwise} \end{cases}. \tag{2.2}$$

As illustrated by Castillo [4], clipping is a non-linear process that produces both in and out of band noise. The existence of the latter becomes apparent as the signal is oversampled. If clipping is performed without proper filtering, other bands would be affected by this out-of-band noise. An option to solve this problem would be to use an analog filter at the output of the signal. Another option, and the one we'll explore here, would be digital filtering through the use of DFTs of zero-padded sequences. Let us consider a sequence of N mapped symbols denoted $(X_k)_{0 \leq k \leq N-1}$. Let us introduce the oversampling factor, J, as a positive integer. The zero-padded sequence would then be

$$X_k^{(\text{zp})} = \begin{cases} X_k & \text{if } k < N \\ 0 & \text{otherwise} \end{cases}, 0 \leq k < JN.$$

After a JN-point IDFT, we get an oversampled discrete time domain representation of the OFDM signal, which is then clipped according to equation 2.2. After clipping, a JN-point DFT is performed and the result becomes

$$X_k^{(\mathrm{cf})} = \begin{cases} \tilde{X}_k & \text{if } k < N \\ \tilde{n}_k & \text{otherwise} \end{cases}, \tag{2.3}$$

where the $\tilde{n}_k$ represent out-of-band noise. These noisy components are removed and the OFDM-modulated sequence is, actually, $\tilde{X}_k$. The following figure shows a transmitter that includes clipping and filtering.

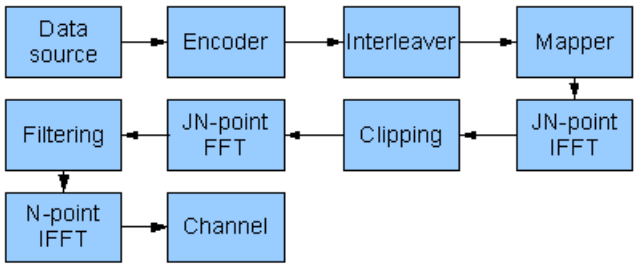

Figure 2.1. Block diagram for an OFDM transmitter that includes oversampling, clipping and filtering as shown on the second row.

The following figure shows the effect of clipping and filtering on the CCDF of the PAPR of an OFDM system.

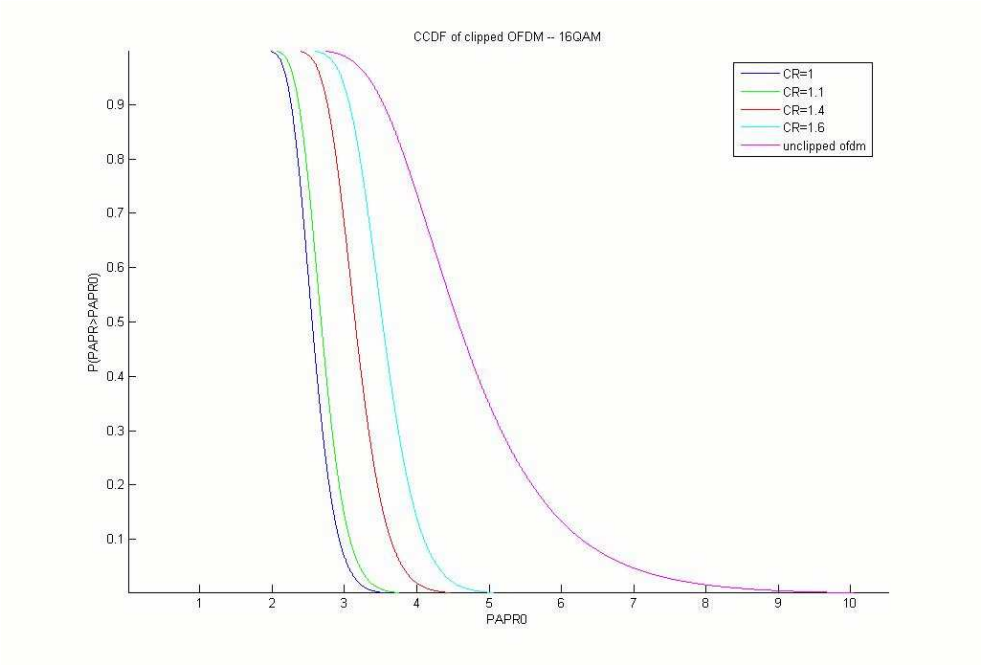

Figure 2.2. CCDF of the PAPR of a clipped and filtered OFDM sequence of symbols. In this figure, there is a total of 64 subcarrier frequencies, and the oversampling factor is equal to 16.

As shown by Armstrong [7], when filtering is performed after clipping a peak regrowth occurs. This explains why the curves in figure 2.2 show that PAPR after clipping and filtering is substantially higher than could be expected from the set value of the CR. For instance, if we set CR=1.6 we obtain a maximum amplitude of $1.6\sqrt{P_{\text{avg}}}$, yielding an expected maximum PAPR of $1.6^2 = 2.56$. From the above figure, it can be easily seen that this is not the case, and that the peak regrowth due to filtering after clipping is quite noticeable. However, PAPR is still greatly reduced even for the more permissive CRs in the figure. This shows that a significant reduction of PAPR is achieved through this technique, yet we still don't know its effects on the system's performance.

2.2 Effects on system performance

First, we must notice that the receiver has not been modified to take into account the effect of clipping and filtering. To see the effects in terms of system performance of clipping and filtering, we can refer to the results of Ochiai and Imai [6] (illustrated in more detail by Castillo [4]), which state that, assuming the incoming sequence X_k is a memoryless and wide-sense stationnary gaussian process, the output of the clipping and filtering process can be modelled statistically as

$$\tilde{X_k} = \alpha X_k + d_k, \tag{2.4}$$

where α is an attenuation and a function of γ,

$$\alpha = 1 - e^{-\gamma^2} + \frac{\sqrt{\pi}}{2}\gamma \text{erfc}(\gamma), \tag{2.5}$$

and d_k is the in-band clipping noise, which cannot be removed through filtering. This result predicts a degradation in performance, as noise *and* attenuation are added to the symbols even before their entrance into the channel. At the channel output we obtain the following expression for the received symbols:

$$Y_k = H_k(\alpha X_k + d_k) + Z_k. \tag{2.6}$$

In this expression, H_k is the channel's k-th frequency response component, which acts directly upon the k-th symbol, and Z_k is Additive White Gaussian Noise (AWGN). From the equations above, we can expect a significant drop in system performance as the CR is set to small values (near 1). These expectations are met as simulations are done on this type of system; the following figure shows this system's performance for different clipping ratios over an AWGN channel.

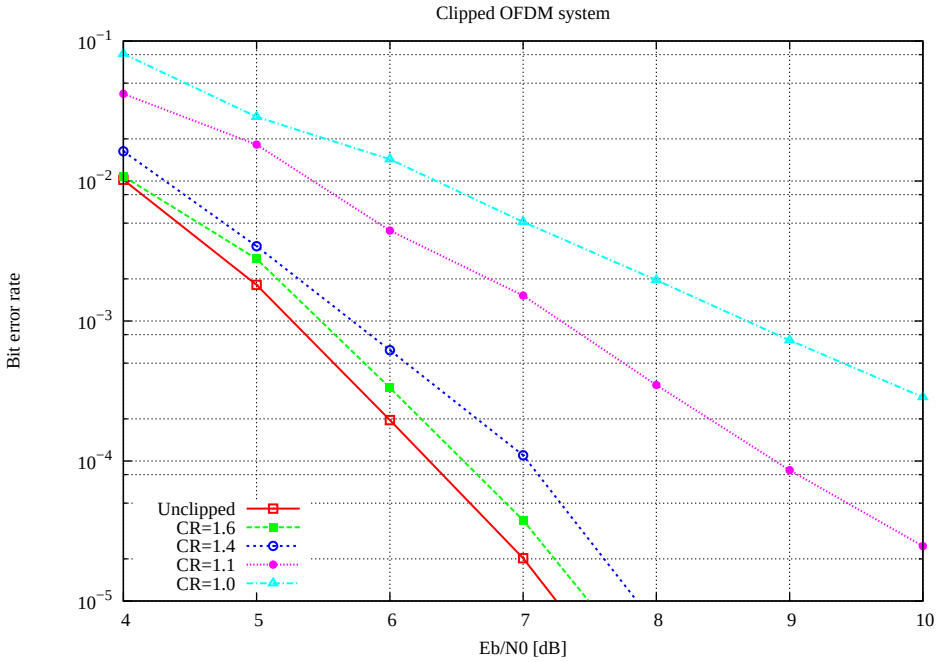

Figure 2.3. System performance for 64 subcarrier frequencies, oversampling factor of 16 and the shown clipping ratios over an AWGN channel. Performance worsens as the clipping ratio is reduced.

In figure 2.3, the signal to noise ratio is recalculated using equation 11 of [6],

$$P_{\text{out}} = (1 - e^{-\gamma^2})P_{\text{in}}, \tag{2.7}$$

for the signal power (γ is, as usual, the clipping ratio). Since the signal is clipped, its power decreases and therefore this reduction must be taken into account when calculating the noise power for the simulation. The validity of this formula, though not shown in this report, has been numerically proven through extensive simulation.

From the results obtained by simulation we can see that we need to find a way to improve system performance when making use of the clipping and filtering technique, since we cannot profit from the reduction in PAPR given by this technique at low CRs if performance is to be damaged so drastically. A series of techniques aiming to solve this problem have been proposed, and in particular, a technique proposed by Chen and Haimovich [8] will be implemented and tested in one of the following chapters.

Chapter 3
Linear precoding

Linear precoding is an important tool for wireless communications since it helps to exploit the channel diversity and therefore it provides a gain in performance when used over the fading channels typical of wireless transmission schemes. In this chapter we will study its effects on an OFDM signal's PAPR, as well as its effects in performance.

3.1 Emitter description

A linearly precoded OFDM emitter is characterized by the following block diagram.

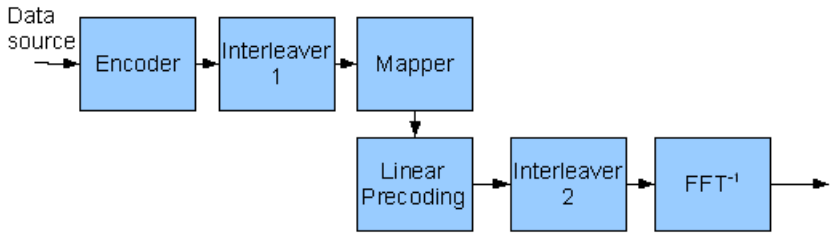

Figure 3.1. A simplified precoded OFDM transmitter. A new interleaver provides added protection against burst errors and minimizes any existent correlation between subsequent symbols.

The Linear Precoding block (LP block) applies a linear transformation on the sequence of mapped symbols. Mathematically speaking, it performs the following operation,

$$\boldsymbol{x}_{\text{out}} = \mathbf{P}\boldsymbol{x}_{\text{in}},$$

where $\mathbf{P}$ is the precoding matrix. Many types of matrices have been proposed with the goal of maximizing the introduced diversity to the OFDM signal. As stated by Le Masson [3], Ma and Giannakis [9] proposed a set of matrices that maximize the diversity gain for a maximum likelyhood decoding scheme, and Goeckel and Ananthaswamy [10] proposed another set of matrices that maximize diversity but constrained to minimizing the PAPR. However, because of their simplicity and fast calculation times due to a technique that resembles the FFT, Hadamard matrices (along with the fast Hadamard transform) are the precoding matrices of choice, even though they are not optimal matrices. On the receiver side, the second interleaver finds its deinterleaving counterpart followed by the most simple possible treatment for linear precoding, which is to perform the matrix operation $\boldsymbol{y}_{\text{out}} = \mathbf{P}^{-1}\boldsymbol{y}_{\text{in}}$, where $\boldsymbol{y}_{\text{in}}$ denotes the deinterleaved message sampled from the channel and $\boldsymbol{y}_{\text{out}}$ is the linearly "decoded" vector. The rest of the receiver is left unchanged.

3.2 A revision of the worst case

Going back to the worst case situation depicted in section 1.2, we seek a mapped symbol sequence $\boldsymbol{x}$ such that

$$\mathbf{P}\boldsymbol{x} = \lambda \boldsymbol{v}, \tag{3.1}$$

where $\boldsymbol{v} = (1, e^{j\phi}, e^{j2\phi}, ..., e^{j(L-1)\phi})^{\dagger}$, L is the precoding matrix size and λ and ϕ are defined as before. For the special case of BPSK, the only possible values of ϕ are 0 and π; for QPSK and 16QAM, the allowed values for ϕ are 0, $\pm\pi/2$ and π.

Considering the particular case of (normalized) Hadamard matrices, defined recursively by $\mathbf{D}$

$$\mathbf{D}_L^H = \frac{1}{\sqrt{L}} \begin{pmatrix} \mathbf{D}_{L/2}^H & \mathbf{D}_{L/2}^H \\ \mathbf{D}_{L/2}^H & -\mathbf{D}_{L/2}^H \end{pmatrix} \tag{3.2}$$

with $\mathbf{D}_1^H = 1$, and consistently defined for $L = 2^K$, it can be shown that the sought vector is given by

$$\boldsymbol{x} = \lambda \mathbf{D}_L^H \boldsymbol{v}, \tag{3.3}$$

since a normalized Hadamard matrix has itself as its inverse. The first component of $\boldsymbol{x}$ is equal to

$$X_1 = \frac{\lambda}{\sqrt{L}} \sum_{n=0}^{L-1} e^{jn\phi} = \begin{cases} \lambda\sqrt{L} & \text{if } \phi = 0 \\ 0 & \text{otherwise} \end{cases}.$$

This result comes from the constraints imposed on the values of ϕ, from the fact that $\sum_{n=0}^{KN-1} e^{\pm j2\pi n/N} = 0$, and from assuming that L is a multiple of 4, that is, that $L = 2^k, k > 1$. This means that when $\phi \neq 0$, the first mapped symbol to be encoded must be equal to zero for the worst case to arrive. This is impossible since all of the elements of the considered constellations are nonzero. On the other hand, a small calculation shows that if ϕ is chosen to be equal to zero, then

$$X_k = \begin{cases} \lambda\sqrt{L} & \text{if } k = 1 \\ 0 & \text{otherwise} \end{cases},$$

which means that *all* of the components except for the first must be equal to zero for this case to arrive, and we've seen that this is impossible. Therefore, the former worst case does not arrive when precoding with a Hadamard matrix symbols from the BPSK, QPSK and 16QAM constellations. We start to notice the additional benefits of linear precoding: the worst case in which the measured PAPR is equal to the number of subcarriers is no longer present, and we might start to suspect that probably linear precoding not only reduces the worst-case PAPR but might also reduce PAPR in general.

3.3 Reduction of PAPR

To show the fact that linear precoding can reduce PAPR, simulations can be done in order to find the CCDF curves for linearly precoded OFDM PAPR. The required simulations were done by Castillo [4], and the resulting CCDF function is presented below. The mapped symbols belong to a 16QAM constellation.

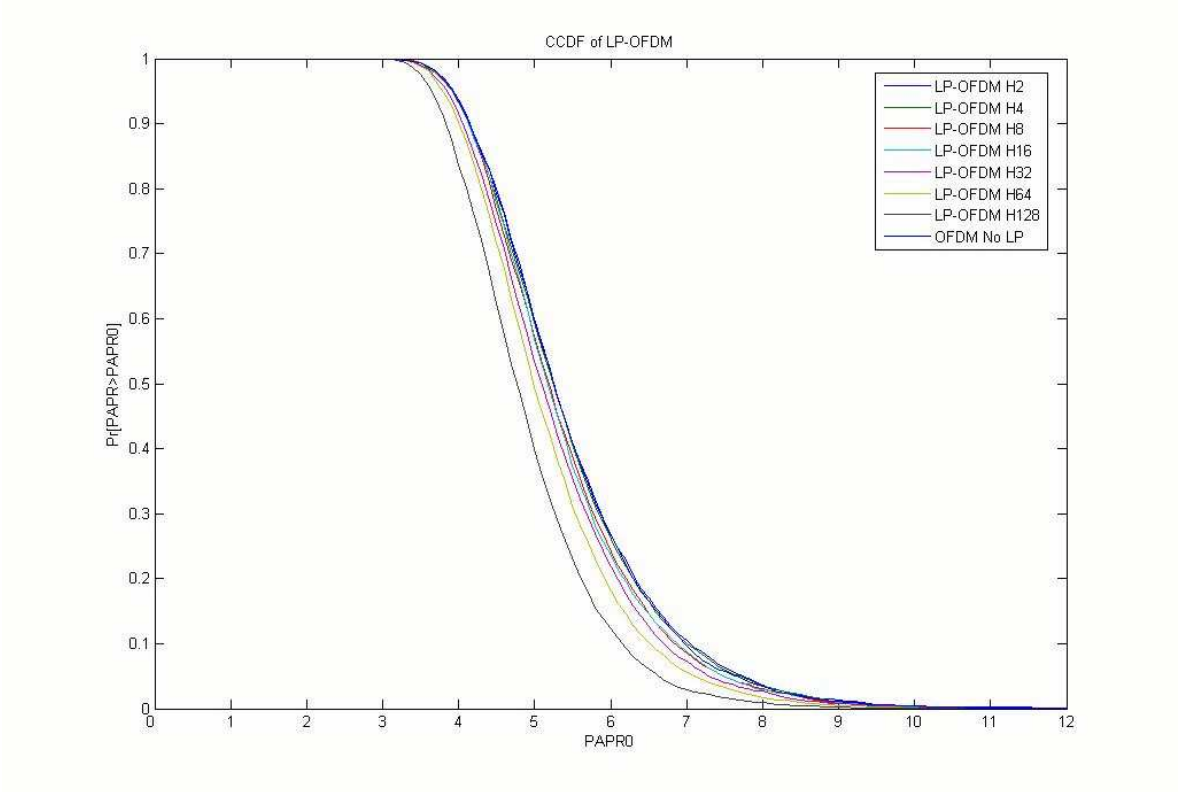

Figure 3.2. CCDF of linearly precoded OFDM PAPR using Hadamard matrices. As seen above, as the precoding matrix is chosen larger, the CCDF curve shifts to the left, showing a reduction of PAPR.

This graph shows the modest reduction in PAPR achieved through the addition of linear precoding. As the matrix size grows larger PAPR is reduced, which confirms the guess we made above when making calculations for the worst case. It is interesting to notice that linear precoding reduces PAPR even though it enlarges the constellation used in the system, as shown in chapter 4 of Castillo. Intuitively speaking, if a larger constellation were to be sent through an OFDM modulation, the resulting signal's amplitude should be increased, but this is not the case. Let us also remember that a matrix product increases the complexity level of the emitter, particularly if the matrix size is chosen fairly large. For this reason, a Hadamard matrix of size 8 will be chosen for all simulations. For this matrix, the following performance was obtained.

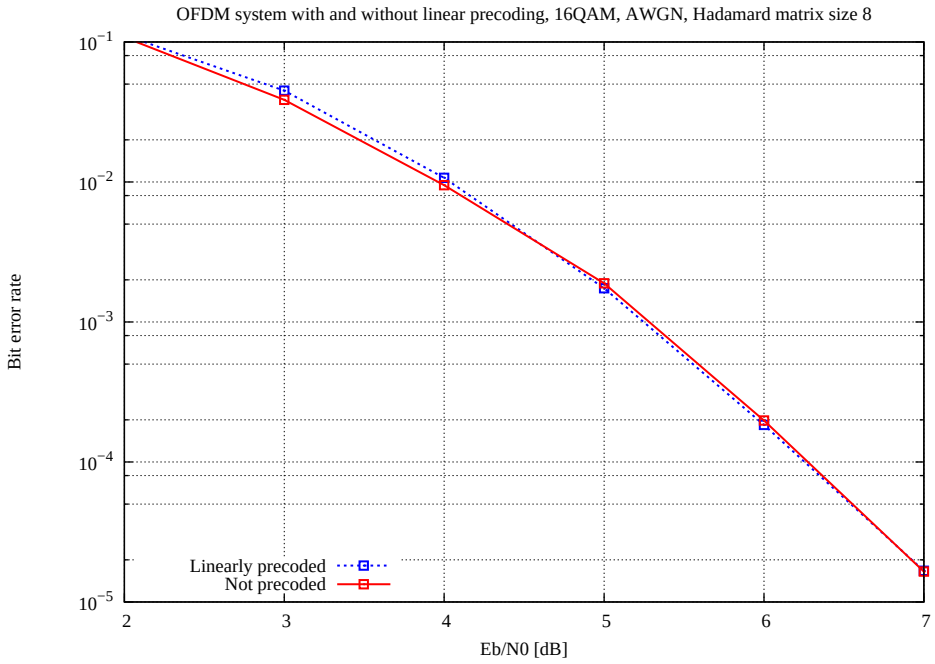

Figure 3.3. OFDM system with and without linear precoding using a Hadamard matrix of size 8 over an AWGN channel.

The obtained performance with linear precoding shows no change when compared to the performance without linear precoding. This result is consistent with the statement that linear precoding is predominantly useful when transmitting through a frequency-selective channel, as mentioned in the introduction. Hence, since the channel used in the figure is AWGN (a non-selective channel), there is no difference at all. However, as shown in, for instance, chapter 3 of [3], this is not the case over fading (Rayleigh) channels. At low values of the Signal to Noise Ratio (SNR), the non-precoded system shows a slightly better performance, while the better performance belongs to the precoded system at larger values of the SNR. Also, the value of the SNR at which a linearly precoded system's performance becomes better than that of a non-precoded system depends on the type of receiver used. As a matter of fact, a precoded system with Minimum Mean Square Error equalization surpasses a non-precoded system at a lower SNR than a system with zero forcing equalization. This can also be seen in [3].

With this final result, we have shown that linear precoding reduces PAPR slightly without damaging the information inside the signal and that at high values of SNR it enhances the communication system's performance slightly. On top of this, we expect an even better performance over a Rayleigh channel, where the real significance of linear precoding, i.e. providing diversity to the sent signal, makes its appearance.

3.4 Clipping and linear precoding

As linear precoding reduces PAPR, and so does the clipping and filtering technique, it seems to be worthwhile to try and use both techniques at the same time. The emitter is represented by the following block diagram.

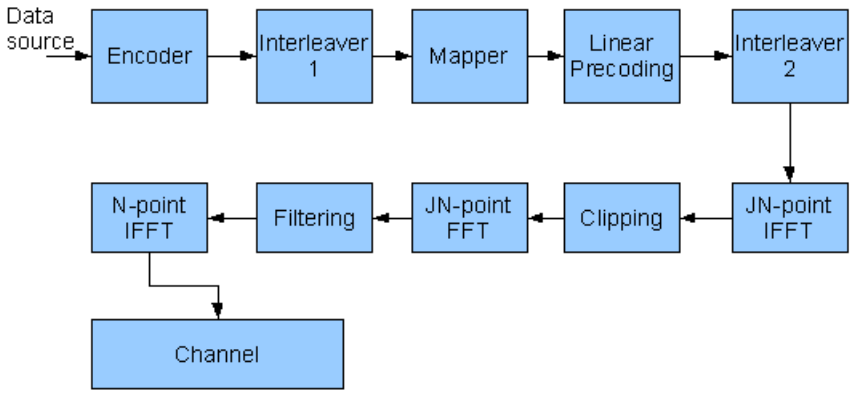

Figure 3.4. Block diagram for an OFDM emitter with clipping, filtering and linear precoding. The receiver is the same as the one used for a linearly precoded OFDM system.

From this system we would expect a slight improvement in performance provided by the linear precoding, since it reduces the PAPR of the OFDM signal and hence the part of the signal severed by the clipping and filtering process should not be as large as in the non-precoded case.

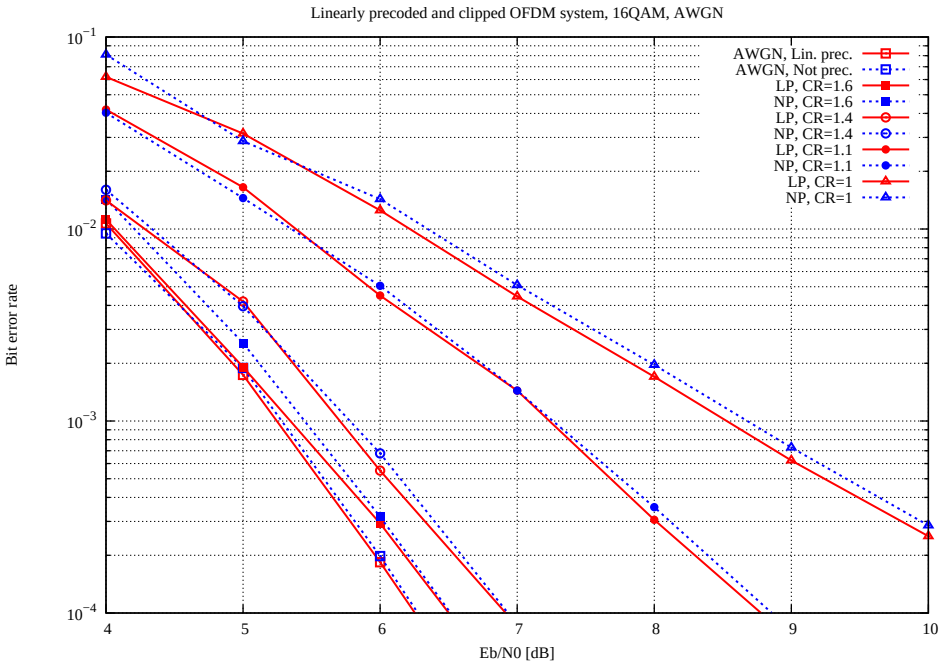

Figure 3.5. Performance of a precoded and clipped OFDM system for a variety of clipping ratios. As mentioned before, the linearly precoded and non-precoded unclipped system's performance curves are identical. They are shown from this point on for the sake of completeness.

Figure 3.5 shows the performance of the system proposed above. The curves on the bottom left region of the graph correspond to the case in which no clipping is performed. As could be expected, the effect of the clipping ratio is still the same: as it becomes smaller, the system performance degradates significantly. However, at sufficiently large SNRs, the curves produced by the linearly precoded system show a slightly better performance than those produced without it, which was expected. However, the question of whether using linear precoding is of real benefit to the system remains, since the improvement in system performance is rather small over AWGN channels. In the following chapter, we will continue testing linear precoding in different situations to see whether it is useful for achieving a better performance.

Chapter 4

An iterative technique for clipped OFDM signals

Several different techniques for boosting a clipped OFDM system's performance have been proposed in the last few years. Castillo [4] focused his work on implementing and testing two techniques whose aim is to minimize the effect of clipping on system performance.

One of them is the Turbo Decision Aided Reconstruction of clipping noise, proposed by Kim and Stuber [11]. The emitter in this case is the same as the one shown in figure 2.1, and the receiver has a main branch consisting of an IDFT, an equalization stage for the channel coefficients, a demapping and deinterleaving stage and a decoding and correcting stage, namely, a decoder for the convolutional (channel) encoding. The reconstruction of the power peaks is done as follows: the originally received and equalized mapped symbol sequence is brought back to the time domain via an IDFT and it is compared to a corrected mapped symbol sequence in the time domain produced using the corrected data from the decoder. A new mapped symbol sequence is then chosen from this comparison. If a time-domain element[4.1] from the corrected sequence has an amplitude higher than that defined by the clipping ratio at the emitter, then the element from the corrected sequence is chosen, and the element from the original sequence is chosen otherwise. Taking the DFT of this new sequence, a new mapped symbol sequence is produced and taken through the process of demapping, deinterleaving and decoding, as with the original sequence, to produce a new corrected mapped symbol sequence and repeat the process until a given number of iterations is reached. A block diagram for this system can be found in [4] and a more formal definition of this technique can be found in [11].

The remarkable issue to point out for this technique is the number of DFTs needed to complete the receiver. To get the mapped symbol sequence from the channel, a DFT is needed; in order to compare the original and corrected symbol sequences in the time domain, two IDFTs are needed, and finally, to get the frequency-domain representation of the newly chosen time-domain element sequence another DFT is needed. The total number of needed DFTs is four. The second technique studied in [4], the Iterative Estimation and Cancellation of clipping noise for OFDM signals (IEC) proposed by Chen and Haimovich [8], needs only

4.1. In this context, the word "element" refers to one of the time-domain samples of the ODFM signal. This distinction is made so that the time-domain samples are not confused with the (frequency-domain) mapped symbols from which the OFDM signal is constructed.

three DFTs, as will be shown below, and Castillo [4] himself showed that both systems achieve similar performances. It is for these reasons that we have chosen to study the performance of a clipped OFDM system with IEC implemented at the receiver. We will now turn to the definition of the receiver.

4.1 The IEC receiver

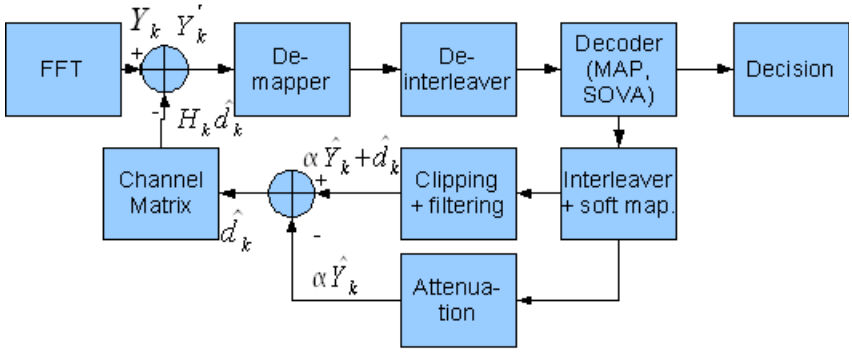

Figure 4.1. IEC-implementing clipped-OFDM receiver. The entrance of information from the channel into the FFT is not shown in the figure.

Figure 4.1 shows the IEC receiver as proposed by Chen and Haimovich [8]. As the incoming signal is brought to the time domain by the FFT shown at the left of the figure, the sequence of received symbols is

$$Y_k = H_k(\alpha X_k + d_k) + Z_k,$$

as it was stated in equation 2.6. As defined before, H_k is the channel coefficient acting on a given subcarrier frequency, α and d_k are the attenuation and noise induced by the clipping process, respectively, and Z_k is AWGN. An estimation of the correct information is made from these received symbols, leading to the decision block on the right. However, since the channel coding used here is convolutional coding, through a MAP or Soft Output Viterbi decoding Algorithm a series of corrected symbols $\hat{X}_k$ can be obtained after interleaving and mapping, as in the emitter. Two branches spawn from the output of the soft mapping block: one of them reproduces the clipping process at the emitter and the other calculates the theoretical attenuation of α introduced by clipping, since it can be calculated from the clipping ratio. These branches yield $\alpha\hat{X}_k + \hat{d}_k$ and $\alpha\hat{X}_k$ respectively. These two results are subtracted and scaled by the channel coefficient H_k, and finally, this result is subtracted from the originally received sequence, yielding

$$Y_k' = Y_k - H_k\hat{d}_k = H_k(\alpha X_k + d_k) + Z_k - H_k\hat{d}_k = H_k(\alpha X_k + d_k - \hat{d}_k) + Z_k. \tag{4.1}$$

Assuming an eventually perfect symbol estimation, $d_k = \hat{d}_k$, and so the clipping noise is perfectly cancelled. The information from which new estimations are done comes from

$$Y_k' = \alpha H_k X_k + Z_k.$$

This seems to be a very powerful result, considering that only three DFTs were used: one for the retrieval of symbols from the channel and two more that are needed for clipping and filtering the estimated symbol sequence. The next step is to test this system's performance, and this will be done in the following section.

4.2 Performance and some modifications

The first test conducted on this system was done over an AWGN channel ($H_k = 1$). Performance was measured for a clipping ratio of 1; encoding is done via a rate 1/2 convolutional code with $(133, 171)_8$ as generating polynomials, the chosen constellation is 16QAM, the oversampling factor for the clipping process is 16 and a Max-Log-MAP algorithm works as the channel decoder. The results are presented below.

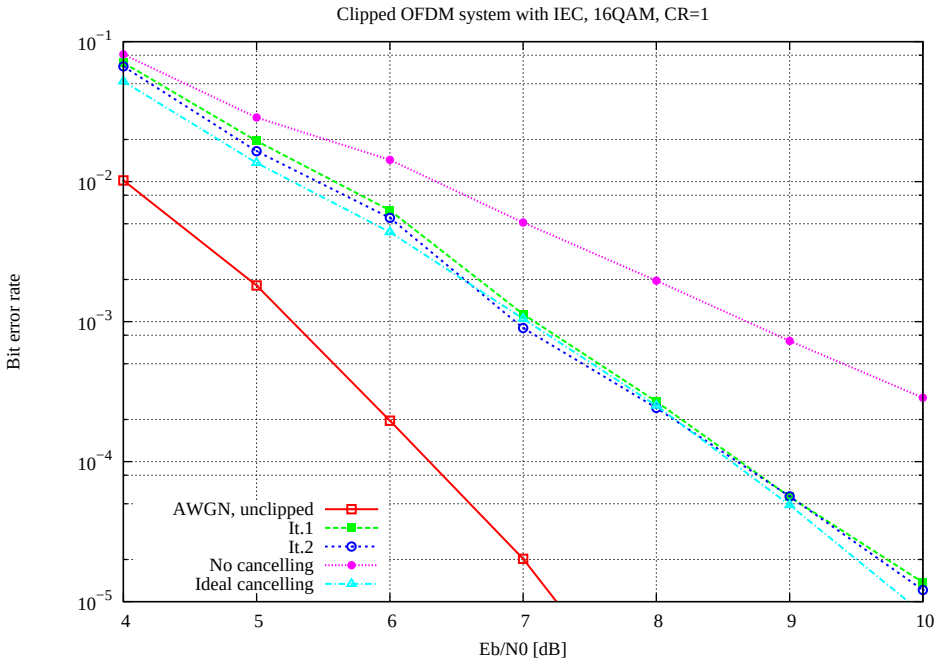

Figure 4.2. OFDM system clipped with CR=1. There is a significant improvement in performance, but the non-clipped system's curve is far from being reached.

The first fact to be noticed from the curves in figure 4.2 is that a significant boost in performance is achieved with only one iteration, and the curve for the second iteration approaches the curve for ideal cancellation as the SNR becomes larger. Furthermore, for SNR>8dB only one iteration is needed, since the curves for both iterations show almost the same performance. However, it is surprising that not even the curve for ideal cancellation approaches the curve for an

unclipped OFDM system. However, we must keep in mind that attenuation plays a role in the decisions made at the receiver for a 16QAM constellation, a problem that should not arise in QPSK nor BPSK. Indeed, since the symbols obtained after ideal cancelling of clipping noise are given in this case by $Y_k^{'} = \alpha X_k + Z_k$, we need to take away the second effect of the clipping process, i.e. attenuation. The simplest solution for this problem would be to perform a zero-forcing equalization at the input of the demapper, that is, to multiply every symbol by α^{-1}. In that case, the noisy symbols corrected by the cancellation technique become

$$Y_k^{'} = H_k\left(X_k + \frac{d_k - \hat{d}_k}{\alpha} \right) + \frac{Z_k}{\alpha}. \tag{4.2}$$

From figure 4.2, we know that the cancellation of clipping noise is quite effective, and hence the second term inside the parentheses in the above equation should not bother the system at the second iteration. The Gaussian noise term, however, will be amplified at smaller values of the CR, and hence we should expect the system performance curve for the ideal cancellation scenario to be parallel and shifted to the right of the unclipped system performance curve. This shifting should be further increased by the fact that, according to eq. 29 of [6], the signal power is written as $P_{\text{tot}} = \alpha^2 P_{\text{sig}} + P_{\text{dis}}$. That is, the total signal power as stated in equation 2.7 is divided into two parts; one of them contains the sent information (and is attenuated by a factor of α^2) and the other contains the distortion provoked by clipping the signal. These two factors should shift the ideal cancellation performance curve to the right in a noticeable manner.

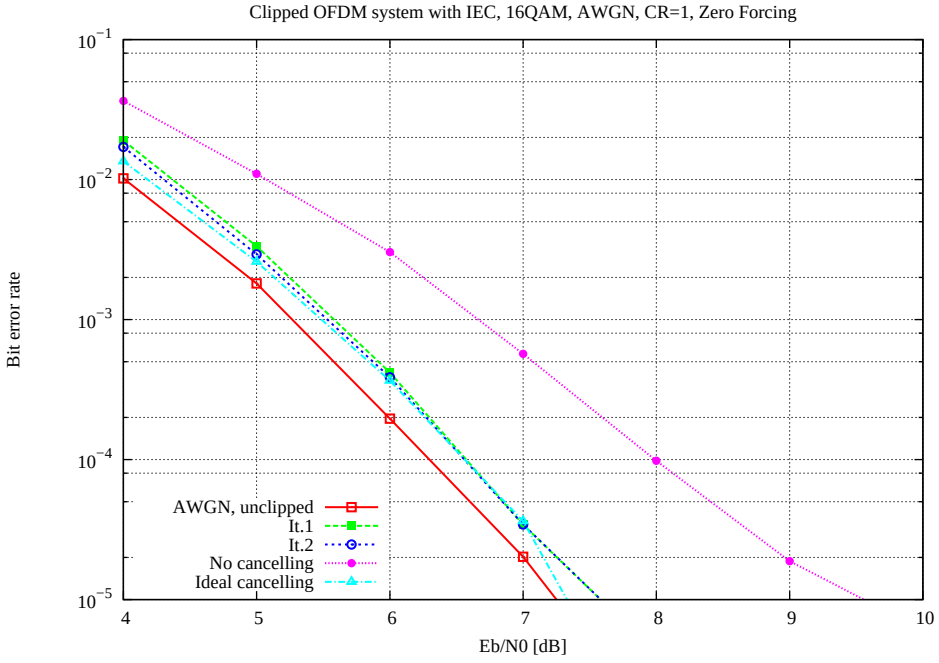

Figure 4.3. Reproduction of the simulation shown in figure 4.2, including zero-forcing equalization.

The results of adding the zero-forcing equalization are shown in figure 4.3. They show that, in terms of performance, this new system is very close to the unclipped one, showing a loss of about 0.3dB in the worst case for the first iteration, and that for SNRs larger than 6dB it is enough to perform only one iteration to obtain a performance reasonably close to the one obtained through ideal cancelling. Also, our predictions on how this system's performance curves would be parallel and shifted to the right of the unclipped case are confirmed. To lessen the amplification done on the gaussian noise term and still perform a proper equalization, a Minimum Mean Square Error equalization could be used instead of zero-forcing. The constant to be multiplied is

$$\frac{\alpha}{\alpha^2 + \sigma_w^2/\sigma_x^2},$$

where σ_w^2 and σ_x^2 are the noise variance and the average power of an equally probable random sequence of constellation elements. In this case, since the constellation used is 16QAM, $\sigma_x^2 = 10$. Using this at the equalization stage yields the following performance.

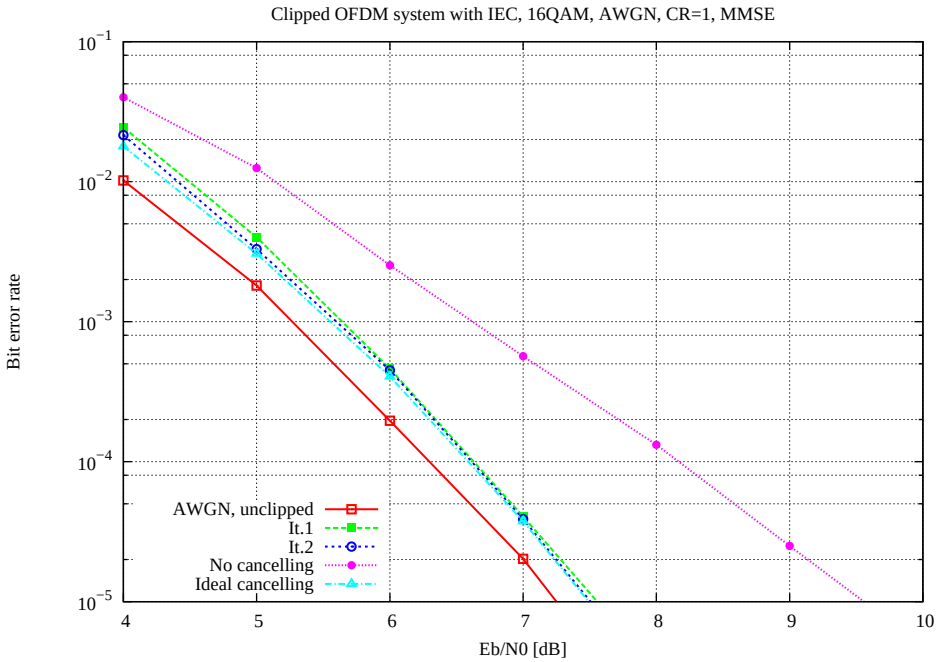

Figure 4.4. A simulation similar to that of figure 4.3, with an MMSE equalization instead of zero-forcing.

There is no visible difference between figures 4.3 and 4.4; the curves obtained seem to have the same behavior and, in fact, when the figures are investigated closely, we find that the better performance belongs to the zero-forcing equalized version of this system, even though it is only a slight advantage.

In the preceding chapter, the benefits of combining clipping and linear precoding were explored. Motivated by the slightly better performance of precoded systems at high SNRs, the above simulations will be reproduced for systems similar to those considered at the above simulations, the only difference being a linear precoding stage consisting of a size 8 Hadamard matrix. The results are shown below.

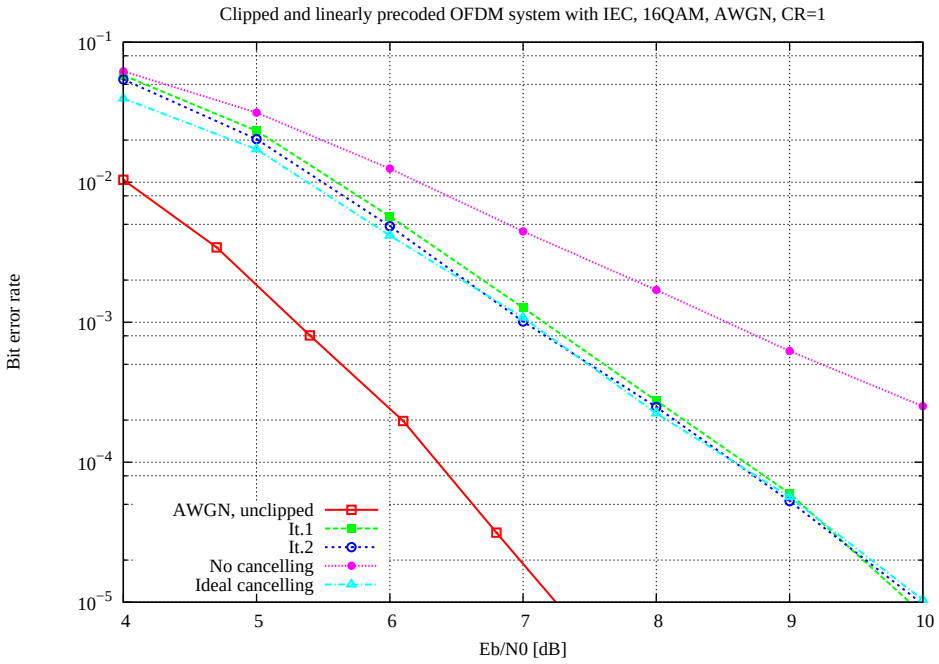

Figure 4.5. Clipped OFDM system with parameters equal to those of fig. 4.2 and including linear precoding.

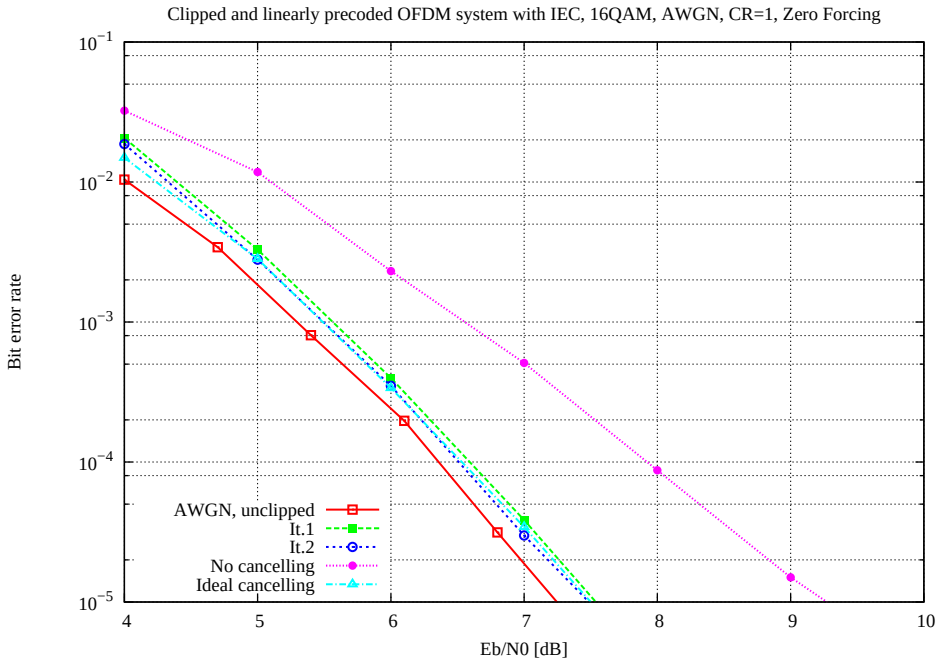

Figure 4.6. Linearly precoded and clipped OFDM system with zero-forcing equalization.

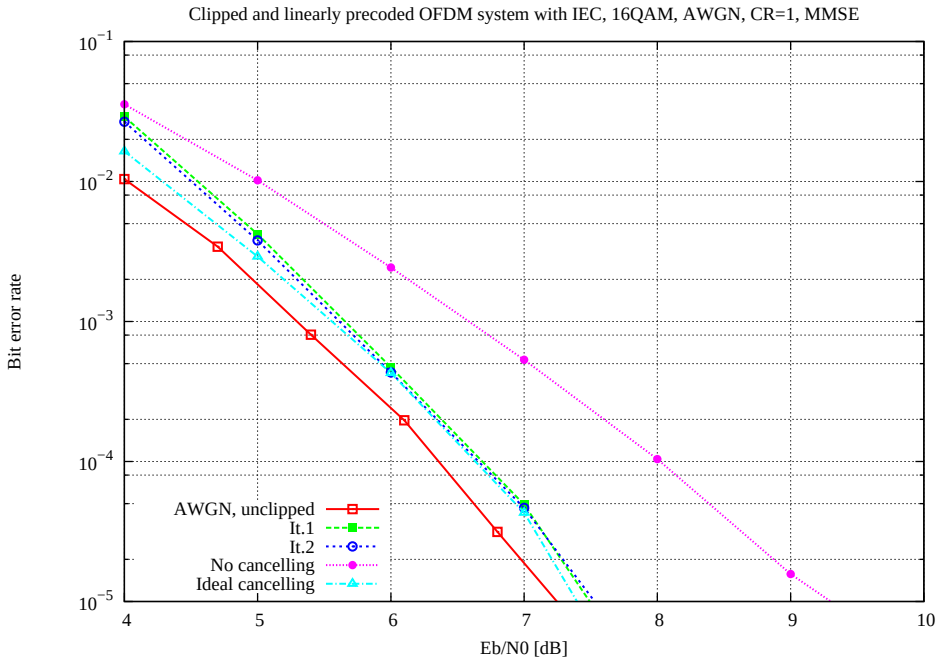

Figure 4.7. Linearly precoded and clipped OFDM system with MMSE equalization.

As might be expected, these results are similar in every way to those without linear precoding except for a slight improvement. This has become customary to this point, given what we already know from linear precoding; since it reduces

slightly the OFDM signal's PAPR, as it is clipped and filtered a lesser amont of the signal is clipped and therefore less information is lost in the process.

It is here where we come to a final improvement to the system in terms of a lower bound for the clipping ratio. Since the noise term is being amplified, we must find a CR such that the attenuation factor α is closer to 1 and that is still low enough to maintain a low PAPR. If we choose a less strict clipping ratio, for instance one of 1.2, then the results are as follows.

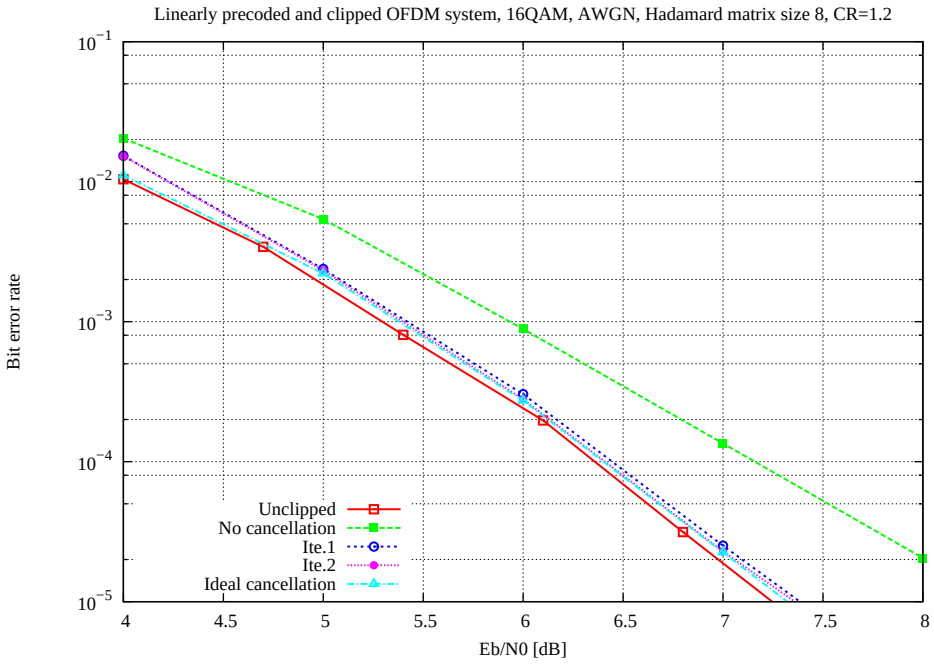

Figure 4.8. A linearly precoded, clipped and zero-forcing equalized OFDM system with clipping ratio equal to 1.2.

For this clipping ratio, and taking advantage of the small boost given by the linear precoding, we find a set of curves that show a loss of around 0.1dB with respect to the unclipped system. Moreover, in the region covered by this plot, it can be seen that for SNRs larger than 5dB only one iteration is needed to obtain a performance quite comparable to the unclipped system. This result, combined with figure 2.2 shows that with the proposed technique PAPR can be held to under a value of 4 and still get a performance close to that of an unclipped system over a Gaussian channel.

As tests have only been done over Gaussian channels, we now turn to a block-fading multipath channel. For the following simulation, a white Rayleigh channel was used and 16 trajectories were considered. The receiver has a zero-forcing equalization for both channel frequency response and clipping attenuation, linear precoding is performed through a size 8 hadamard matrix and the mapped symbols belong to a 16QAM constellation. IEC is implemented at the receiver. The results are presented below.

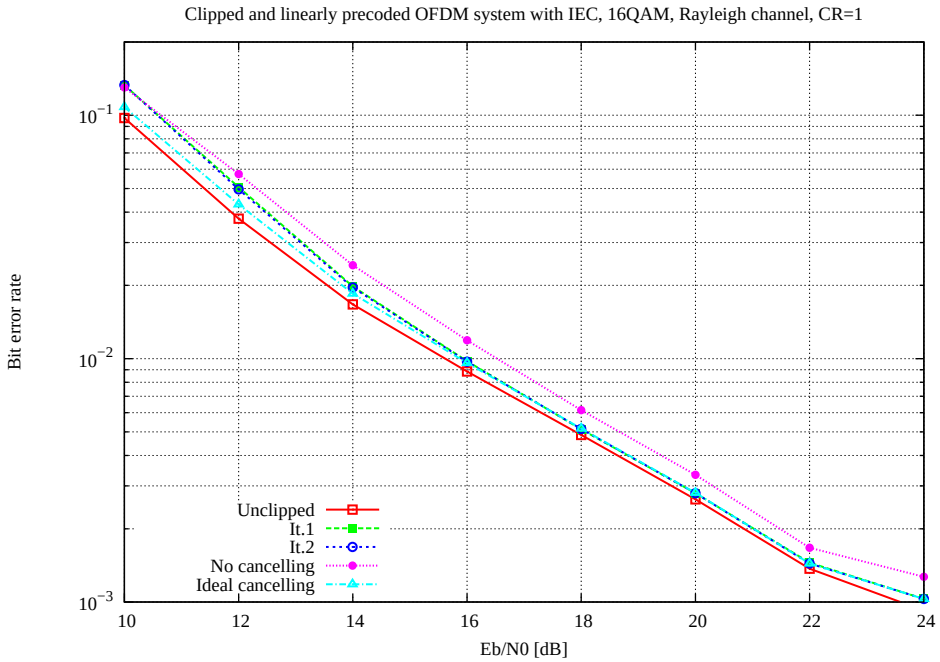

Figure 4.9. Clipped OFDM system with linear precoding, IEC and zero forcing equalization over a 16-path white Rayleigh channel. The clipping ratio is set to 1.

Though at the time of completion of this report there were still a number of problems with the simulation[4.2], some information can still be extracted from figure 4.9. To start with, we can point out that the loss due to clipping and filtering is of about 1dB at the low SNR region of the graph and slowly decreases to about 0.6dB at the bottom right corner of the figure. This means that at a sufficiently high signal to noise ratio, the loss due to clipping is not as radical as before, when testing over a Gaussian channel. Secondly, there seems to be no improvement over the first IEC iteration when two of them are done. Though there is still a difference between the curves of the first and second iterations and the ideal cancellation curve at low SNRs, it seems that further iterations are unimportant if we wish to improve the system's performance. Finally, at SNRs larger than 16dB the curves for the two iterations and the ideal cancellation of clipping noise coincide. This means that for sufficiently high SNRs it is not necessary to do more than one iteration, since the upper bound for the IEC system performance has already been achieved. Finally, as stated in section 4.2, we find a small but inevitable difference between the unclipped system and the ideal cancelling system curves that comes from clipping and that results in noise amplification and useful signal power attenuation.

4.2. The problems encountered here were related with the unclipped system performance. As the curve on the bottom left corner of figure 4.9 was compared with a series of reference curves, it was not possible to fully validate the system's performance, hence making these results only partially valid. Future work is to be undertaken on this simulation to present valid results on its totality.

4.3 A clipped system with iterative treatment of linearly precoded OFDM

Le Masson [3] proposed an iterative scheme for linearly precoded OFDM. This system's transmitter is the same as in figure 3.1, while the receiver is the one shown in figure 4.10.

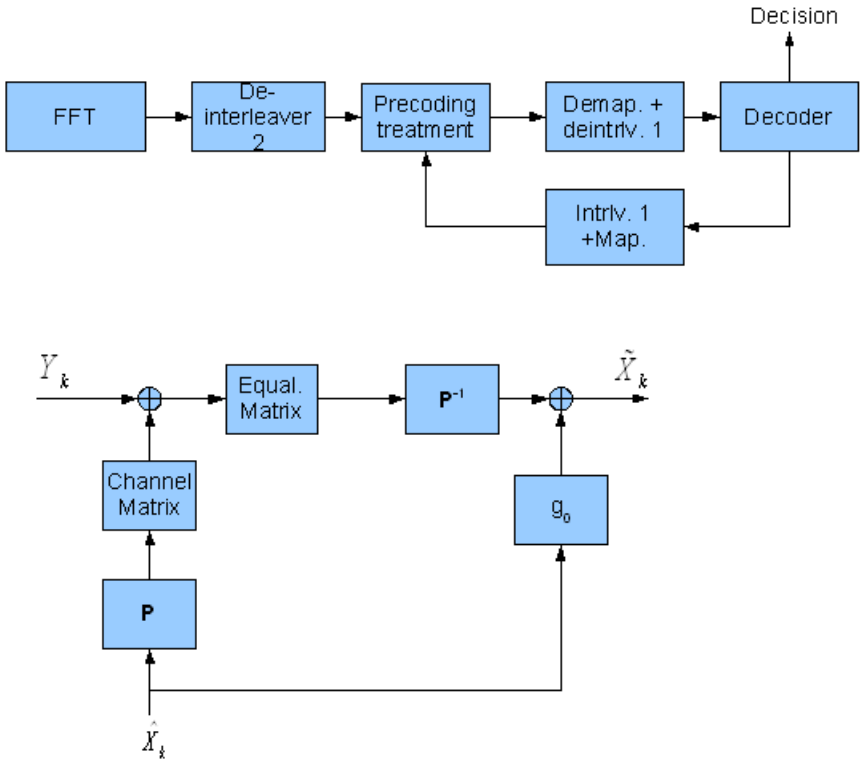

Figure 4.10. Block diagram of Le Masson's OFDM receiver with iterative treatment of linear precoding. Above is the general block diagram, and as before, the entrance from the channel into the FFT block is omitted. Below is the definition of the precoding treatment block; inputs and outputs in this figure correspond to those in the general block diagram.

The core of this system is the precoding treatment block. It receives a non-equalized, deinterleaved and linearly precoded symbol sequence (Y_k) and an estimated symbol sequence coming from the decoder block through an interleaving and soft mapping blocks ($\hat{X}_k$) to return a new corrected linearly precoded symbol sequence ($\tilde{X}_k$). Each block inside the precoding treatment is defined below, as stated in [3].

$$g_0 = \frac{1}{L}\sum_{k=0}^{L-1} q_k h_k \tag{4.3}$$

$$q_k = \lambda \frac{h_k^\star}{(\sigma_x^2 - \hat{\sigma}_x^2)|h_k|^2 + \sigma_w^2} \tag{4.4}$$

$$\lambda = \frac{\sigma_x^2}{1 + \beta\sigma_{\hat{x}}^2} \tag{4.5}$$

$$\beta = \frac{1}{L}\sum_{k=0}^{L-1}\left|\frac{h_k}{\alpha_k}\right|^2 \tag{4.6}$$

$$\alpha_k = \left((\sigma_x^2 - \hat{\sigma}_x^2)|h_k|^2 + \sigma_w^2\right)^{1/2} \tag{4.7}$$

The channel attenuation coefficients h_k can be represented through a diagonal matrix, $\mathbf{H}$. The equalization matrix $\mathbf{Q}$ is diagonal as well and has q_k as its elements. These are defined by h_k, λ, σ_w^2, σ_x^2 and $\sigma_{\hat{x}}^2$. The last three variances are the noise variance, the transmitted symbol variance assuming that all symbols appear with the same probability, and the estimated symbol variance calculated from the estimated symbols coming from the decoding block. λ is defined in the equations above.

This receiver was tested along with a clipped and linearly precoded OFDM emitter. The precoding was performed using a size 8 Hadamard matrix, the channel is a WLAN channel that includes 16 trajectories and a doppler shift corresponding to a speed of 30m/s and 5 iterations were performed[4.3]. The parameters for the channel encoder and decoder are the same as those used before.

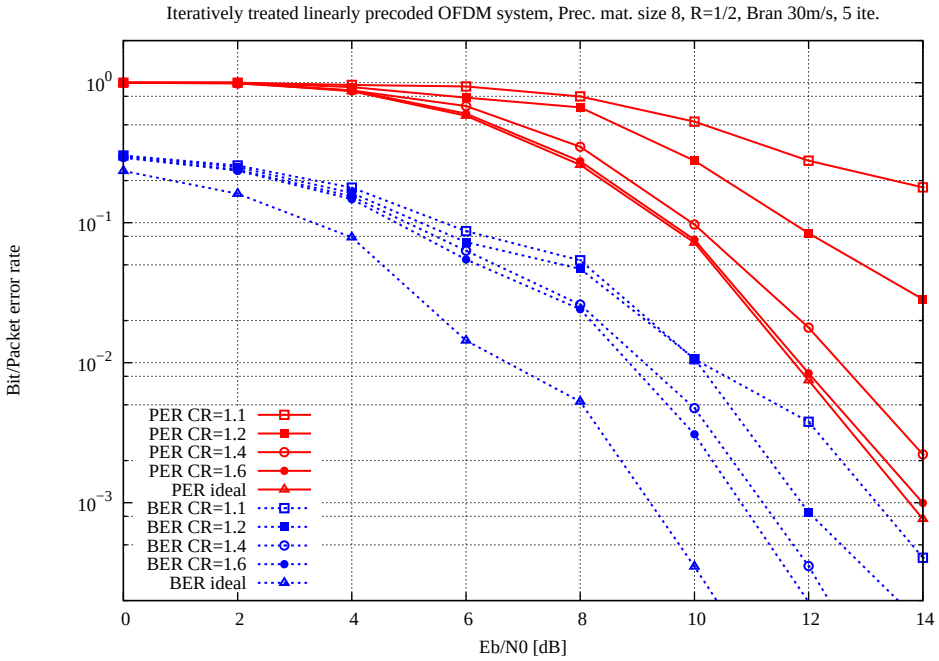

Figure 4.11. Clipped and precoded OFDM transmitter tested with J. Le Masson's iterative linear precoding treatment receiver over a multipath fading channel. Packet error rates worsen as the CR drops below 1.6.

In figure 4.11, performance curves for this receiver are shown for a variety of clipping ratios. Ideal cancelling curves were calculated for a system without clipping. It is noticeable that performance in terms of PER seems to be significantly damaged only for clipping ratios of less than 1.6. However, for this same value of

4.3. Let us note that in this case the number of iterations is counted from the first made decision, that is, the decision made without any a-priori information is the first iteration, while in the case of IEC this was the zero-th iteration.

the clipping ratio, the BER is significantly more damaged. This is to be expected, however, since one packet error means *at least* one bit error in the package. Therefore, the same number of *packets* is damaged with or without clipping at CR=1.6, while the damaged *bits* are certainly greater.

4.4 Comments

In this chapter, a pair of iterative methods were tested with the purpose of using the clipping technique while trying not to damage the communication system's performance.

The first method, Chen and Haimovich's IEC [8], yielded impressive results over a Gaussian channel, leaving the system's performance untouched at CR=1.2 when used along with linear precoding. However, its performance over a multipath fading channel is still a partial unknown, and considering that the IEC technique is mainly focused on removing the clipping noise at the receiver, the gain obtained through the use of linear precoding could be almost negligeable. As a matter of fact, only a zero forcing equalization was used as treatment for the linear precoding at the emitter, and as shown in [3], this could become an obstacle rather than an advantage. Over a multipath fading channel, zero forcing is the equalization scheme that requires the largest SNR in order to overcome a non-equalized system's performance, and therefore we would like to have a proper equalization scheme to enhance IEC and obtain a better performance.

The second method, Le Masson's iterative treatment of linear precoding, has a very powerful precoding treatment scheme that could solve the IEC technique's equalization problem. However, it is only oriented in that direction, and not toward the problems introduced by clipping in themselves. It does show a slight robustness to clipping, as linearly precoded systems have a better performance when clipped than non-precoded systems, as shown in chapter 3.

From the results of this chapter, it can be seen that it is desirable to find a system that implements a combination of the two systems in order to make use of the benefits of both iterative precoding treatment and iterative estimation and cancellation of clipping noise.

Conclusions and future work

In this work, the problem of PAPR in OFDM systems was outlined, and a first approach toward controlling the maximum PAPR in these systems was carried out through the use of the clipping and filtering technique ([7], [6]). The main strength of this technique is the radical reduction of PAPR that can be achieved. However, its use also brings degradation in the system's performance, since clipping produces attenuation and noise that make the correct detection of sent symbols a difficult task, particularly for small values or CR.

Linear precoding was the next topic taken into consideration, noting its PAPR reducing capabilities and its benefits when used over a multipath channel ([10], [3], [9]). Its main drawback is the addition of complexity on both the emitter and the receiver, but since it reduces PAPR modestly and exploits the channel diversity it becomes a useful tool for recovering the OFDM system performance when clipping the sent signal.

A combination of the two was considered, and it was concluded that a system that includes clipping and filtering combined with linear precoding yields a better performance than one that includes only clipping. Conversely, it yields lower values of PAPR than one including only linear precoding.

As the following step, two iterative techniques were tested for a linearly precoded and clipped sent signal. One of them, IEC ([8]), showed promising results over a Gaussian channel, but its performance over a multipath Rayleigh channel is not yet clear, and it lacks a proper treatment of linear precoding. The second, an iterative treatment of linear precoding ([3]), shows a notable robustness against clipping over a multipath channel even though it includes no system to treat the effects of clipping.

The results obtained point toward a system that includes both kinds of iterative treatments, that is, the one used for clipping noise plus the one oriented toward treating linear precoding. Both systems being iterative, a combination of the two can be implemented quite naturally.

In figure 1, a system with these characteristics is proposed. It is composed of a main branch equal to that of the receiver proposed in [3], but two loops are formed by the precoding treatment branch and the IEC branch. This system is very complex in appearance, yet the results obtained from each of the techniques are quite promising, and this complexity could pay off if the resulting performance is close enough to that of an unclipped system for a given number of iterations.

Also, the fact that IEC achieves an acceptable performance two iterations after the first decision raises some doubts on whether both loops should run the same number of iterations. This is because the iterative precoding treatment needs four iterations after the first decision to achieve a performance close to that of an ideal precoding treatment scheme (as shown in [3]). Considering the fact that the corrected symbol sequence coming from the decoder is used by both iterative branches, one might be inclined to think that both loops should run for the largest amount of iterations found between the two (that is, four after the first decision). This is only speculation, however, and a conclusive answer should be found through a complete performance simulation.

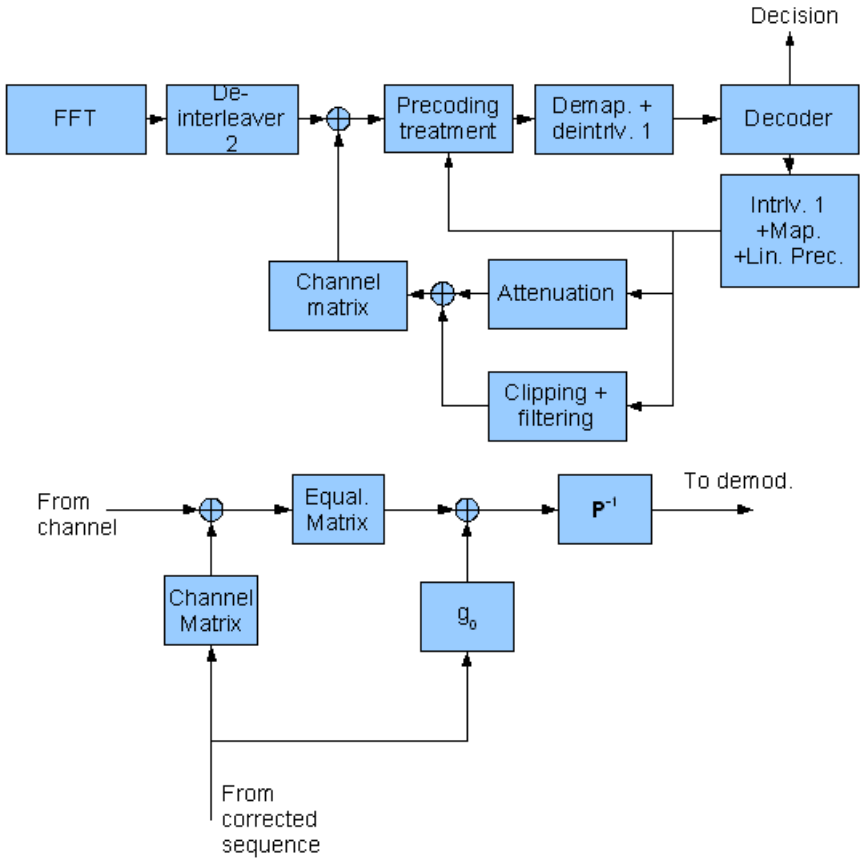

Figure 1. Linear precoding treatment as proposed in [3] combined with the IEC technique proposed in [8]. Equalization for the attenuation provoked by clipping is not presented. The above block diagram shows the general structure of the detector, and the block diagram below shows a modified precoding treatment designed to work alongside the IEC branch.

As a final comment, in this work two iterative techniques were tested and evaluated according to their primary strengths and weaknesses after an extensive study of the PAPR problem and of the use of linear precoding and the problems therein. After this, a new iterative system has been proposed, and future work on this area should focus on its performance and on whether the system's complexity is worth the work of implementing it.

Bibliography

[1] A. R. S. Bahai and B. R. Saltzberg. *Multi-carrier digital communications : theory and applications of OFDM*. Kluwer Academic Pub. Plenum Press, 1999.

[2] J. Boutros and E. Viterbo. Signal space diversity: A power and bandwidth efficient diversity technique for the Rayleigh fading channel. *IEEE Trans. Inform. Theory*, 44:1453–1467, 1998.

[3] J. Le Masson. *Systèmes de Transmission avec Précodage Linéaire et Traitement Itératif - Application à l'OFDM et aux Techniques MIMO*. PhD thesis, ENST Bretagne, Université de Bretagne Occidentale, Brest, France, 2005.

[4] M. Castillo. The peak power problem in OFDM and linearly precoded systems, 2005. Internship report, ENST Bretagne, Universidad de Los Andes.

[5] S. H. Han and J. H. Lee. An overview of peak-to-average power ratio reduction techniques for multicarrier transmission. *IEEE Wireless Comm.*, pages 56–65, april 2005.

[6] H. Ochiai and H. Imai. Performance analysis of deliberately clipped OFDM signals. *IEEE Trans. Comm.*, 50:89–101, 2002.

[7] J. Armstrong. Peak-to-average power reduction for OFDM by repeated clipping and frequency domain filtering. *Elect. Lett.*, 38:246–247, 28th feb. 2002.

[8] H. Chen and A. M. Haimovich. Iterative estimation and cancellation of clipping noise for OFDM signals. *IEEE Comm. Lett.*, 7:305–307, 2003.

[9] X. Ma and G. B. Giannakis. Full-diversity full-rate complex-field space-time coding. *IEEE Trans. Sig. Proc.*, 51:2917–2930, nov. 2003.

[10] D. L. Goeckel and G. Ananthaswamy. On the design of multidimensional signal sets for OFDM systems. *IEEE Trans. Comm.*, 50:442–452, 2002.

[11] D. Kim and G. L. Stüber. Clipping noise mitigation for OFDM by decision-aided reconstruction. *IEEE Comm. Lett.*, 3:4–6, 1999.